EasyChair Preprint

№ 997

1/f Noise: Branching Process Model (II), Computer Simulations

Takayuki Kobayashi

June 24, 2020

$1/f$ Noise : Branching Process Model (Ⅱ) ; Computer Simulation

Takayuki Kobayashi
e-mail : jokyoji@gmail.com

Abstract : Computer simulations are used to test how the branching process model is available to discuss the $1/f$ problem with the equations described in my previous paper, in which a particle may branch into several particles, be absorbed or be observed by a detector. In this work it is assumed that exactly two particles are produced by a branching. The simulations demonstrate that the power spectrum of a series formed by time intervals between successive detections of particles is characterized by a $1/f$ distribution in a wide range of frequency (more than seven decades) when a branching rate of a particle is equal to an absorption rate of the particle in the medium. When the branching rate is less than the absorption rate, the power spectrum turns off from a $1/f$ distribution in a lower frequency-range.

1. Introduction

The mathematical expressions for generating time series of events are given in the previous work[1] by using the branching process model. For a medium in which a particle may be subjected to absorption and branching reactions, the conditional probability $P_k(n,t)$ that n particles are found in the medium at time $t>0$ after we had k particles at $t=0$ in the presence of random particles immigration with the rate S is given in Ref. (1) as

$$P_k(n,t)=\sum_{i=0}^{n} K_k^{(n-i)} Q_0^{(i)}, \tag{1-1}$$

where $K_k^{(n-i)}$ and $Q_0^{(i)}$ are the contribution of the k particles in the medium at $t=0$ and of the particle immigrating into the medium during the time interval (0, t), respectively. They are given here again.

$$K_k^{(n-i)}=\sum_{l=0}^{n-i} p(l,t) K_{k-1}^{(n-i-l)}, \tag{1-2}$$

and

$$K_0^{(i)}=\delta_{i,0}. \tag{1-3}$$

When the multiplication rate of a particle μ and the parameter α are defined as

$$\mu=\lambda_m/\lambda_a \text{ and } \alpha=\lambda_a-\lambda_m=(1-\mu)\lambda_a, \tag{1-4}$$

where λ_a and λ_m are the absorption and branching rates, respectively, of a particle, the function $p(n,t)$ for the case of binary branching process in Eq. (1-2) is given as

$$p(n,t)=\begin{cases} W_1 & (n=0) \\ \left(\dfrac{1-\mu}{1-\mu e^{-\alpha t}}\right)^2 e^{-\alpha t} & (n=1), \\ \mu W_1 \cdot p(n-1,t) & (n\geq 2) \end{cases} \tag{1-5}$$

in the case of $\mu \neq 1$ (subcritical case), and

$$p(n,t)=\begin{cases} W_2 & (n=0) \\ \left(\dfrac{W_2}{\lambda_a t}\right)^2 & (n=1), \\ W_2 \cdot p(n-1,t) & (n\geq 2) \end{cases} \tag{1-6}$$

in the case of μ =1 (critical case). Here, the functions W_1 and W_2 are defined, respectively, as

$$W_1=\frac{1-e^{-\alpha t}}{1-\mu e^{-\alpha t}}, \tag{1-7}$$

and

$$W_2=\frac{\lambda_a t}{\lambda_a t+1}. \tag{1-8}$$

The contribution of the particle immigration $Q_0^{(i)}$ is obtained as, when $\mu \neq 1$

$$Q_0^{(i)}=\begin{cases} \exp\left[\dfrac{S}{\mu\lambda_a}\ln\dfrac{1-\mu}{1-\mu e^{-\alpha t}}\right] & (i=0) \\ \dfrac{\frac{S}{\mu\lambda_a}+i-1}{i}\mu W_1 \cdot Q_0^{(i-1)} & (i\geq 1) \end{cases}, \tag{1-9}$$

and when μ =1

$$Q_0^{(i)}=\begin{cases} \exp\left[-\dfrac{S}{\lambda_a}\ln(1+\lambda_a t)\right] & (i=0) \\ \dfrac{\frac{S}{\lambda_a}+i-1}{i}\mu W_2 Q_0^{(i-1)} & (i\geq 1) \end{cases}. \tag{1-10}$$

The existing particle number in every time interval αt $(\mu \neq 1)$ or $\lambda_a t$ $(\mu = 1)$ was generated successively using the probability described by Eq. (1-1). The generation of the time series for existing particle number was started from the initial particle number N_0=100. In order to avoid the possibility of the particle number increasing to infinity or dying out, the random immigration rate was chosen to be $S = \alpha N_0$ when $\mu < 1$ (subcritical case), considering the mean number of particles at $t \to \infty$ is S/α[2], and S=0 when $\mu = 1$ (critical case). If $S > 0$ in a critical system, the mean particle number will increase with time and diverge eventually to infinity. The power spectral density (PSD) in case of $\mu = 1$ is shown in Fig. 1, where the series was analyzed using the fast Fourier transformation technique (FFT) with the size of series of 67108864 points, and behaves clearly like f^{-2} over seven decades of frequency f. The PSD seems to deviate from the f^{-2} line in

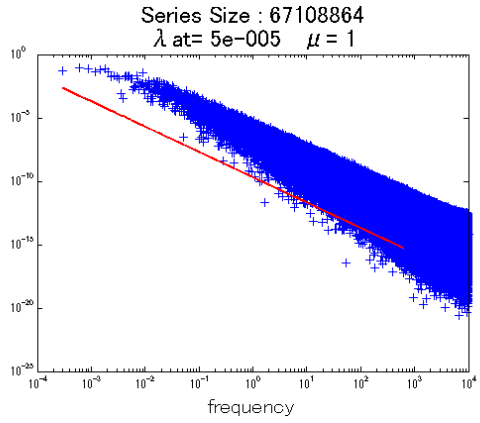

Fig. 1. The PSD of the time series in case of $\mu = 1$. The straight line gives the f^{-2} behavior.

a low-frequency range lower than about $2\text{x}10^{-3}$. Here, time is measured in unit of $1/\lambda_a$ (mean lifetime of a particle absorbed in the medium).

Four examples of the PSD in case of $\mu < 1$ are shown in Fig. 2. In all these cases the PSD converges to a finite value in a low-frequency range, while it holds the f^{-2} behavior in the high-frequency range. The transition frequency from the f^{-2} behavior to the finite-values is around 0.2 in all the cases, i.e. the multiplication rate μ has almost no influence on the transition frequency. The f^{-2} behavior in the high-frequency range reflects the fact that the particle number at a time t_1 may have a determinant influence on the particle number at a following time t_2 even when $\mu = 0.1$, i.e. the correlation between the particle numbers at t_1 and t_2 is strong for a short time interval $t_2 - t_1$ and weak for a long time interval (at frequencies lower than the transition frequency). The results in Figs. 1 and 2 show that the correlation between the particle numbers turns weak after a time interval of only several mean lifetimes by absorption (transition frequency : ~0.2) at $\mu < 1$ but the particle numbers have strong correlation even after several hundreds of the mean lifetime at $\mu = 1$ (transition frequency : ~2 $\text{x}10^{-3}$).

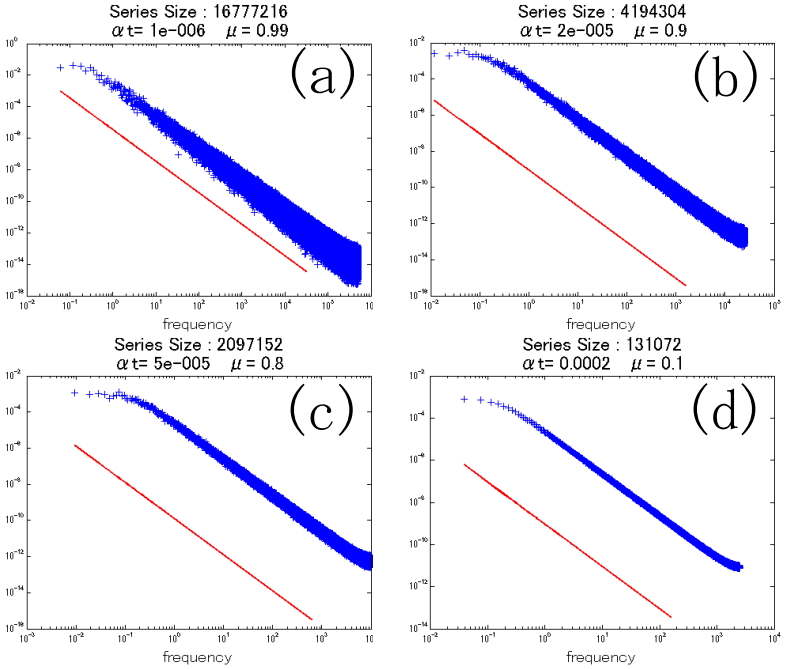

Fig. 2. The PSD of the time series for existing particle number for the cases that: (a) $\mu = 0.99$; (b) $\mu = 0.9$; (c) $\mu = 0.8$ and (d) $\mu = 0.1$. The straight lines give the f^{-2} behavior

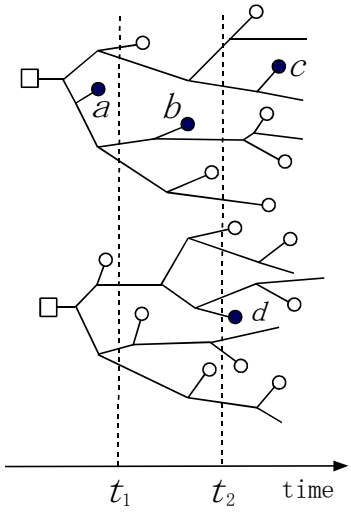

Fig. 3. Chain of the branching processes. The boxes, circles and black spots represent a particle immigrating randomly, absorption and detection of a particle, respectively. The paths (loci) of the particles are shown by full lines. The existing particle number at time t_1 and t_2 are 7 and 11, respectively.

It was noticed in the above analysis that the PSD of time series described by the number of particles existing in a medium behaves like f^{-2}, in a wide range of frequency, due to strong correlations between the particle numbers. It is, however, expected that time intervals between successive incidents occurring in the medium have comparatively weak correlations each other and

the PDS of a series formed by these intervals behaves like $f^{-\gamma}$ $(0 < \gamma < 2)$ as explained in Fig. 3 where detections of a particle are considered.

A detection may correlate with another detection through branching paths as the detections *a*, *b* and *c* in Fig. 3. The detection *d* has no correlation with *a*, *b* and *c*, because it appears in a branching chain originating from a particle immigration different from that for the detections *a*, *b* and *c*. The length of the path between the detections has statistical correlation with the physical time interval. For example, the time interval between *a* and *b* is approximately equivalent to that between *b* and *c*, but, owing to the fact that the path between *b* and *c* is longer than that between *a* and *b*, the correlation between *b* and *c* may be far weaker than that between *a* and *b*. These considerations motivate an analysis of a series formed by time intervals between two successive detections of a particle.

2 Detection probability of a particle

It is rather complicated, even in the case of binary branching, to give the general form of the probability $P_k(m,n,t)$ that *m* counts have been recorded by a detector placed in the medium during the time interval (0, *t*) and *n* particles are found in the medium at time $t > 0$ after we had *k* particles at $t = 0$ [(1)]. In the case that $m = 0$, however, the probability $P_k(0,n,t)$ for binary branching is described closely by a similar form to Eq. (1-1) as[(1)]

$$P_k(0,n,t) = \sum_{i=0}^{n} K_k^{(0,n-i)} \cdot R_0^{(0,i)}, \tag{2-1}$$

and, again as in Fig. (1-1), $K_k^{(0,n-i)}$ and $R_0^{(0,i)}$ are the contribution of the *k* particles in the medium at $t = 0$ and that of the particle immigrating into the medium during the time interval (0, *t*), respectively. The contribution of particles in the medium at $t = 0$, $K_k^{(0,n-i)}$, is described as

$$K_k^{(0,n-j)} = \sum_{l=0}^{n-j} p(0,l,t) K_{k-1}^{(0,n-j-l)} \tag{2-2}$$

$$K_0^{(0,j)} = \delta_{j,0},$$

where

$$p(0,n,t) = \begin{cases} \eta_0 \xi_0 V & (n=0) \\ \frac{(\eta_0 - \xi_0)^2 e^{-\theta_0 t}}{(\eta_0 - \xi_0 e^{-\theta_0 t})^2} & (n=1). \\ V \cdot p(0,n-1,t) & (n \geq 2) \end{cases} \tag{2-3}$$

Here

$$V = \frac{1 - e^{-\theta_0 t}}{\eta_0 - \xi_0 e^{-\theta_0 t}}, \tag{2-4}$$

and

$$\eta_0 = \frac{\lambda_t + \theta_0}{2\lambda_m}, \qquad \xi_0 = \frac{\lambda_t - \theta_0}{2\lambda_m}. \tag{2-5}$$

The parameters θ_0, η_0 and ξ_0 in Eqs. (2-3), (2-4) and (2-5) are given differently depending to the type of the detector of particles. We take two types of the detector into consideration; one is the

detector of absorption type in which a particle is absorbed by detection, and the other of non-absorption type in which the particle counting has no influence on the particle number. We define here λ_d, which is the detection rate of a particle, and λ_c, which is the capture rate of a particle in the medium in addition to the absorption by the detector, and then the absorption rate λ_a and total rate λ_t are given by

$$\lambda_a = \begin{cases} \lambda_c + \lambda_d & (\text{absorption type}) \\ \lambda_c & (\text{non}-\text{absorption type}) \end{cases}, \text{ and } \lambda_t = \lambda_a + \lambda_m, \tag{2-6}$$

and then the multiplication rate μ and the detection rate ε of a particle are described, respectively, as

$$\mu = \frac{\lambda_m}{\lambda_a} = \begin{cases} \frac{\lambda_m}{\lambda_c+\lambda_d} & (\text{absorption type}) \\ \frac{\lambda_m}{\lambda_c} & (\text{non}-\text{absorption type}) \end{cases}. \tag{2-7}$$

and

$$\varepsilon = \frac{\lambda_d}{\lambda_a} = \begin{cases} \frac{\lambda_d}{\lambda_c+\lambda_d} & (\text{absorption type}) \\ \frac{\lambda_d}{\lambda_c} & (\text{non}-\text{absorption type}) \end{cases}. \tag{2-8}$$

By using these parameters, θ_0, η_0 and ξ_0 are expressed, respectively, as

$$\theta_0 = \begin{cases} \lambda_a\sqrt{(1-\mu)^2+4\varepsilon\mu} & (\text{absorption type}) \\ \lambda_a\sqrt{(1+\varepsilon+\mu)^2-4\mu} & (\text{non}-\text{absorption type}) \end{cases}, \tag{2-9}$$

$$\eta_0 = \begin{cases} \frac{1}{2\mu}\left(1+\mu+\sqrt{(1-\mu)^2+4\varepsilon\mu}\right) & (\text{absorption type}) \\ \frac{1}{2\mu}\left(1+\varepsilon+\mu+\sqrt{(1+\varepsilon+\mu)^2-4\mu}\right) & (\text{non}-\text{absorption type}) \end{cases}, \tag{2-10}$$

and

$$\xi_0 = \begin{cases} \frac{1}{2\mu}\left(1+\mu-\sqrt{(1-\mu)^2+4\varepsilon\mu}\right) & (\text{absorption type}) \\ \frac{1}{2\mu}\left(1+\varepsilon+\mu-\sqrt{(1+\varepsilon+\mu)^2-4\mu}\right) & (\text{non}-\text{absorption type}) \end{cases}. \tag{2-11}$$

The other factor $R_0^{(0,i)}$ in Eq. (2-1) is given by

$$R_0^{(0,i)} = \begin{cases} \exp\left[(\xi_0-1)St + \frac{S}{\mu\lambda_a}\ln\frac{\eta_0-\xi_0}{\eta_0-\xi_0 e^{-\theta_0 t}}\right] & (i=0) \\ \frac{\frac{S}{\mu\lambda_a}+i-1}{i}\cdot V\cdot R_0^{(0,i-1)} & (i\geq 1) \end{cases}. \tag{2-12}$$

Using Eqs. (1-1) and (2-1), the probability that the detector counts particles during the time interval (0, t) and n particles are found in the medium at $t>0$ after we had k particles at $t=0$ is given by

$$\sum_{m=1}^{\infty} P_k(m,n,t) = P_k(n,t) - P_k(0,n,t). \tag{2-13}$$

When the probability given by Eq. (2-13) is much smaller than $P_k(0,n,t)$, the probability recording more than two counts may be negligible and the following relation holds approximately:

$$P_k(1,n,t) \doteqdot P_k(n,t) - P_k(0,n,t). \qquad (2\text{-}14)$$

3. Computer simulations

Whether a particle detection has occurred or not in a very short time interval was decided successively by using Monte Carlo method with the probabilities described by Eqs. (1-1), (2-1) and (2-14), from which another series (count series) formed by the time intervals between successive detections was obtained. The random immigration rate S was chosen in a similar way to the time series for the existing particle number. A part of the count series is shown in Fig. 4 in comparison with the series for particle number. The count series has a much more intermittent property than the other.

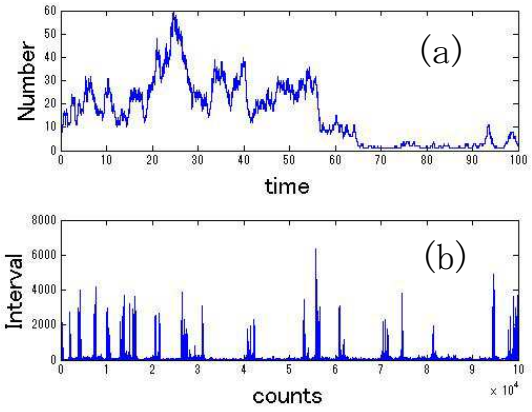

Fig. 4. (a) Time series for existing particle number for $\mu = 1$. (b) Count series for $\mu = 1$ and $\varepsilon = 1$.

3.1 Absorption-type detector

3.1.1 Case of $\mu = 1$ and $\varepsilon = 1$

The FFT results for several sizes of series are shown in Fig. 5. When the series size is shorter than 1048576, the PSD behaves like f^{-1} over five decades of frequency, here the frequency is related to detection counts and not to time. The PSD for the series size over 2097152 begins to deviate from the f^{-1} line in a low-frequency range. This deviation becomes more striking as the series size is longer and the PSD converges to a finite value in a low-frequency range. In all the case, the PSD converges to a finite value in a high-frequency range.

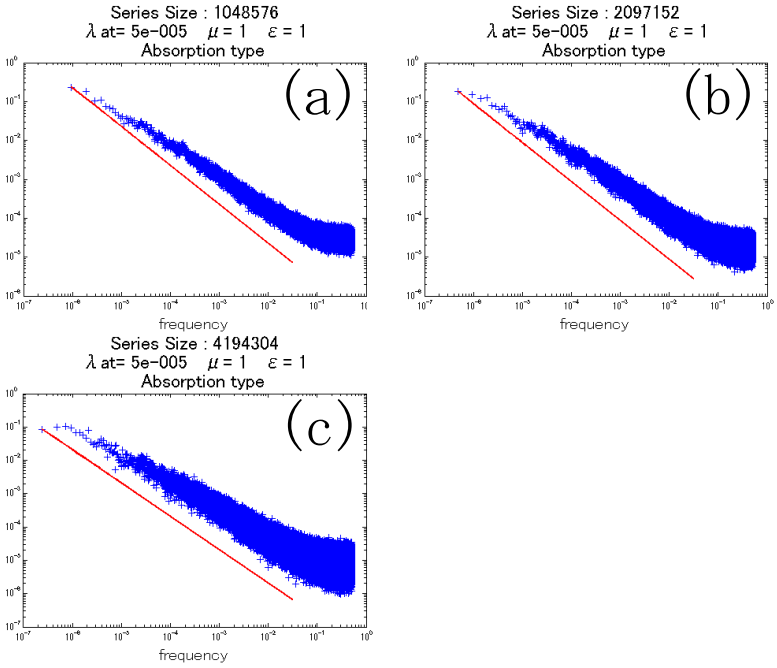

Fig. 5. The PSD of the count series with an absorption-type detector for the case of $\mu = 1$ and $\varepsilon = 1$. The series sizes are (a) 1048576, (b) 2097152 and (c) 4194304, respectively. The straight lines give the f^{-1} behavior.

3.1.2 Case of $\mu = 1$ and $\varepsilon < 1$

The FFT results for $\varepsilon = 0.5$ and 0.1 with $\mu = 1$ are shown in Fig. 6. In case of $\varepsilon = 0.5$, the PSD

Fig. 6. The PSD of the count series for the cases that $\mu = 1$, $\varepsilon = 0.5$ and the series size of (a) 524288 and (b) 1048576, and that $\mu = 1$, $\varepsilon = 0.1$ and the series size of (c) 6536 and (d) 131072, respectively. The straight lines give the f^{-1} behavior.

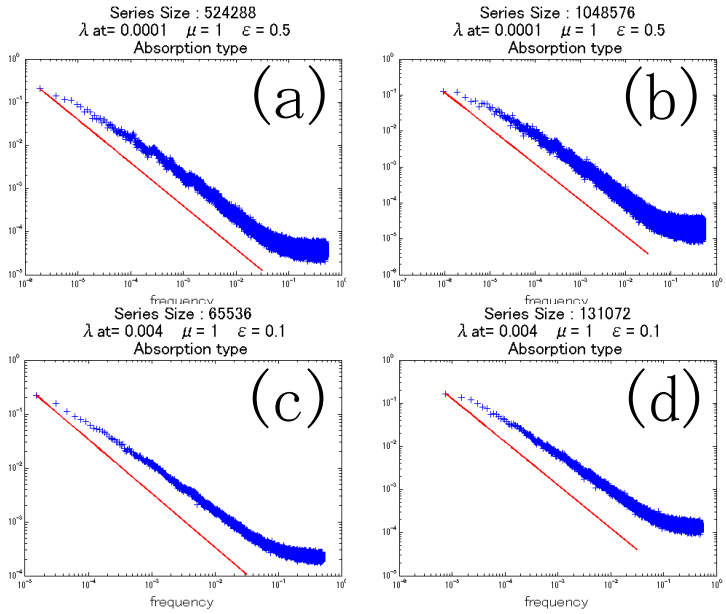

Fig. 7. The PSD of the count series with an absorption-type detector for the case of $\mu = 0.99$ and $\varepsilon = 1$. The series sizes are (a) 131072, (b) 262144 and (c) 524288, respectively. The straight lines give the f^{-1} behavior.

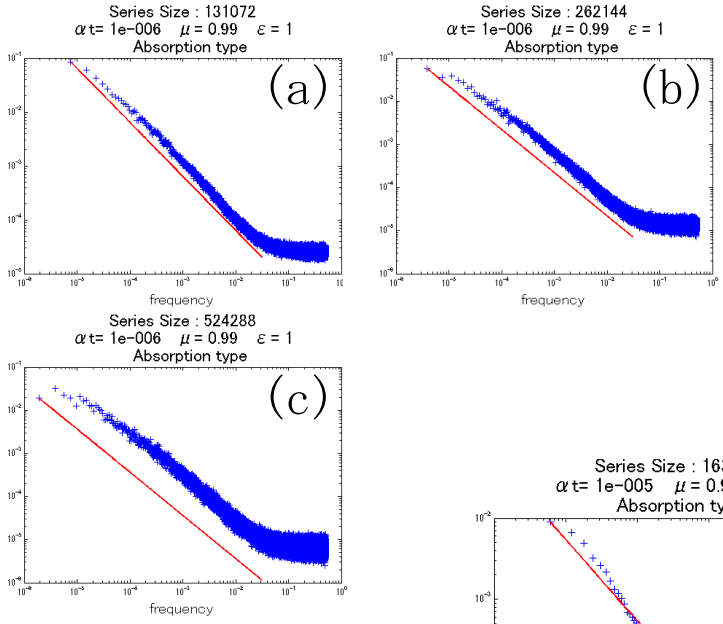

Fig. 8. The PSD of the count series for the cases that $\mu = 0.9$, $\varepsilon = 1$ and the series size of (a) 16384 and (b) 32768, and that $\mu = 0.8$, $\varepsilon = 1$ and the series size of (c) 4096 and (d) 8192, respectively. The straight lines give the f^{-1} behavior.

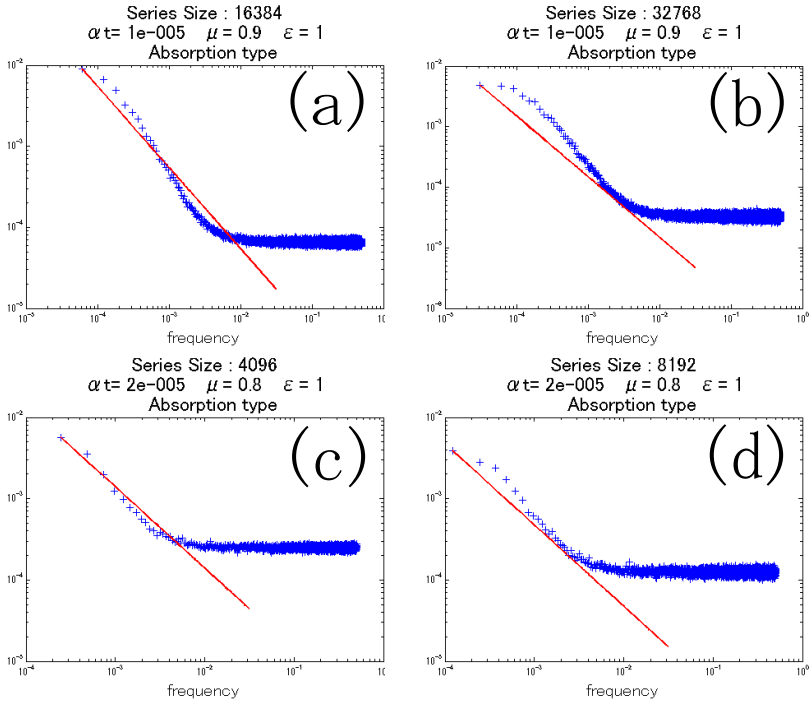

with the series size smaller than 524288 behaves like f^{-1} in a low-frequency range, but it begins to deviate from the f^{-1} line when the series size is 1048576, and this deviation becomes more striking for longer series sizes. The deviation of the PSD from the f^{-1} behavior in a low-frequency range starts at a shorter series size in case of lower detection efficiency ε as shown in Fig. 6(c) and (d).

3.1.3 Case of $\mu < 1$ and $\varepsilon = 1$

The FFT results for $\mu = 0.99$ with $\varepsilon = 1$ are shown in Fig. 7. When the series size is shorter than 131072, the PSD behaves like f^{-1} for more than three decades of frwquency, but the PSD for the series size of 262144 begins to deviate from the f^{-1} line in a low-frequency range and it comes to light for the series with sizes over 524288. This deviation from the f^{-1} behavior becomes remarkable with decreasing the parameter μ as can be seen in Fig. 8 where the FFT results for $\mu = 0.9$ and 0.8 with $\epsilon = 1$ are shown.

When $\mu = 1$, the PSD behaves like f^{-1} for about five decades of frequency as can be seen in Fig. 5, but this frequency range with the f^{-1} behavior decreases to about three decades in case of $\mu = 0.99$ and becomes much more narrower down to only one decade in cases of $\mu = 0.9$ and 0.8.

3.2 Non-absorption-type detector

The PSD of count series with a non-absorption-type detector was estimated in a similar way to the cases with an absorption-type detector.

3.2.1 Case of $\mu = 1$ and $\varepsilon = 1$

The FFT results for two sizes of series are shown in Fig. 9. The PSD behavior is very similar to the case with an absorption-type detector in Fig. 5, and it deviates from the f^{-1} line in a low-frequency range when the series size is over 4194304. The PSD behaves like f^{-1} for five decades or more of frequency which is slightly wider than the case with an absorption-type detector.

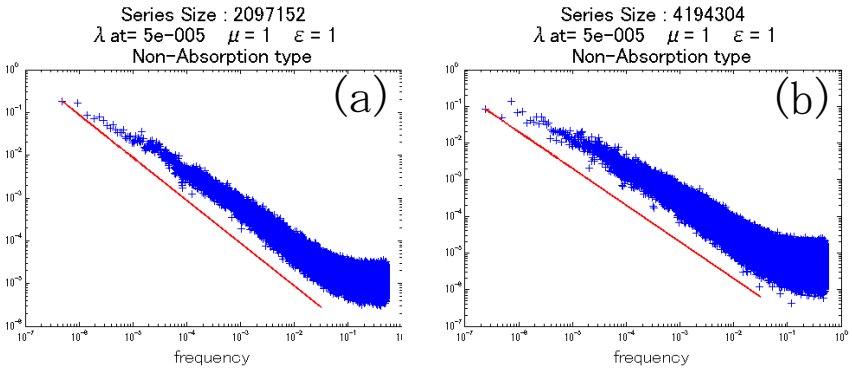

Fig. 9. The PSD of the count series with a non-absorption-type detector for the case of $\mu = 1$ and $\varepsilon = 1$. The series sizes are (a) 2097152 and (b) 4194304, respectively. The straight lines give the f^{-1} behavior.

3.2.2 Case of $\mu = 1$ and $\varepsilon < 1$, and Case of $\mu < 1$ and $\varepsilon = 1$

The PSD's with a non-absorption-type detector for the cases of $\mu = 1$ and $\varepsilon < 1$ and of $\mu < 1$ and $\varepsilon = 1$ are shown in Figs. 10, 11 and 12. These results are also very similar to the cases with an absorption-type detector shown in Figs. 6, 7 and 8.

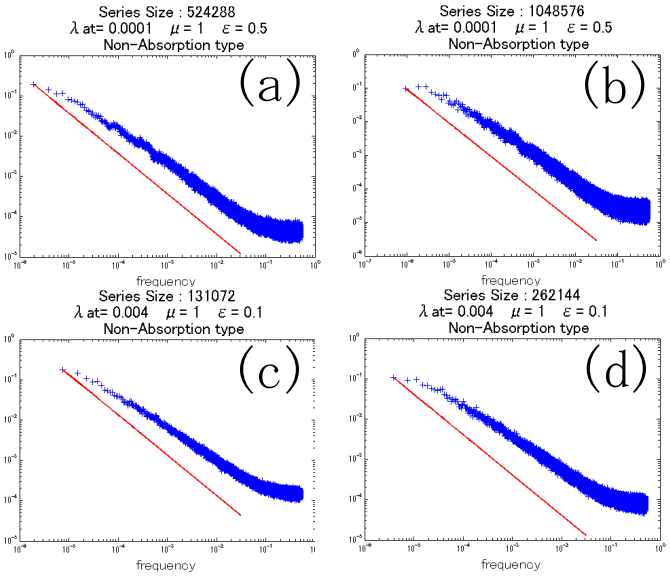

Fig. 10. The PSD of the count series for the cases that $\mu = 1$, $\varepsilon = 0.5$ with the series sizes of (a) 524288 and (b) 1048576, respectively, and that $\mu = 1$, $\varepsilon = 0.1$ with the series sizes of (a) 131072 and (b) 262144, respectively. The straight lines give the f^{-1} behavior.

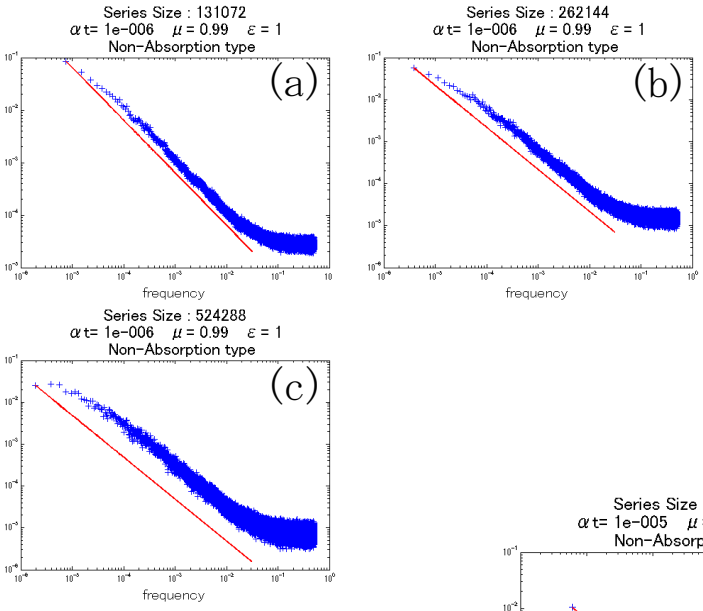

Fig. 11. The PSD of the count series with an non-absorption-type detector for the case of $\mu = 0.99$ and $\varepsilon = 1$. The series sizes are (a) 131072, (b) 262144 and (c) 524288, respectively. The straight lines give the f^{-1} behavior.

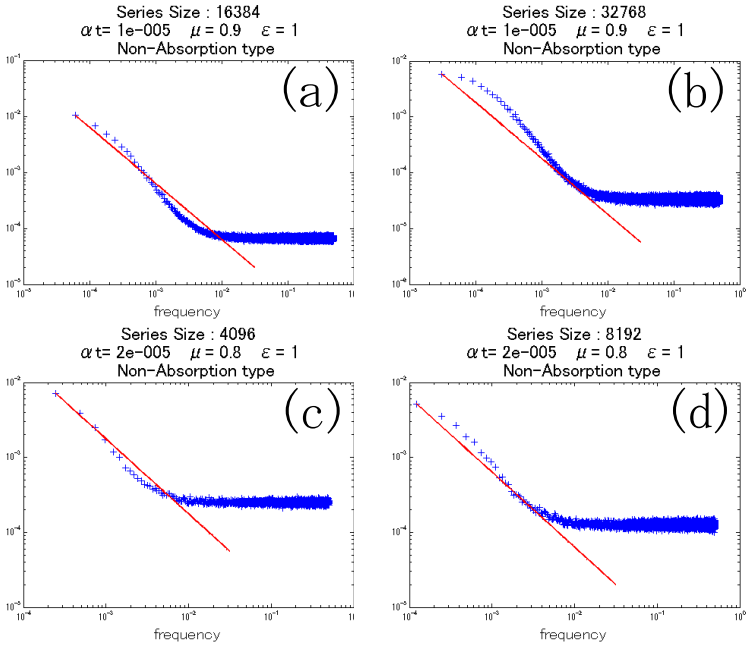

Fig. 12. The PSD of the count series for the cases that $\mu = 0.9$, $\varepsilon = 1$ with the series sizes of (a) 16384 and (b) 32768, respectively, and that $\mu = 0.8$, $\varepsilon = 1$ with the series sizes of (c) 4096 and (d) 8192, respectively. The straight lines give the f^{-1} behavior.

3.2.3 *Case of* $\mu = 1$ *and* $\varepsilon > 1$

When the detector is of non-absorption type, the parameter ε larger than one is possible. The PSD for $\mu = 1$ and $\varepsilon = 2$ is shown in Fig. 13. In this case, $\varepsilon = 2$, each particle is detected twice, on average, before absorbed in the medium. The spectrum is very similar to the case of $\varepsilon = 1$ shown in Fig. 9.

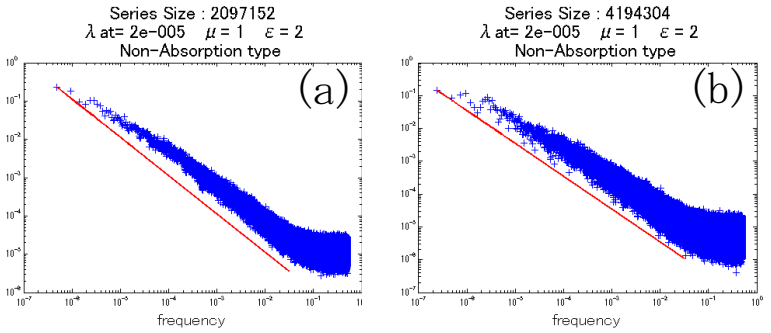

Fig. 13. The PSD of the count series with a non-absorption-type detector for the case of $\mu = 1$ and $\varepsilon = 2$. The series sizes are (a) 2097152 and (b) 4194304, respectively. The straight lines give the f^{-1} behavior.

4. Results and discussions

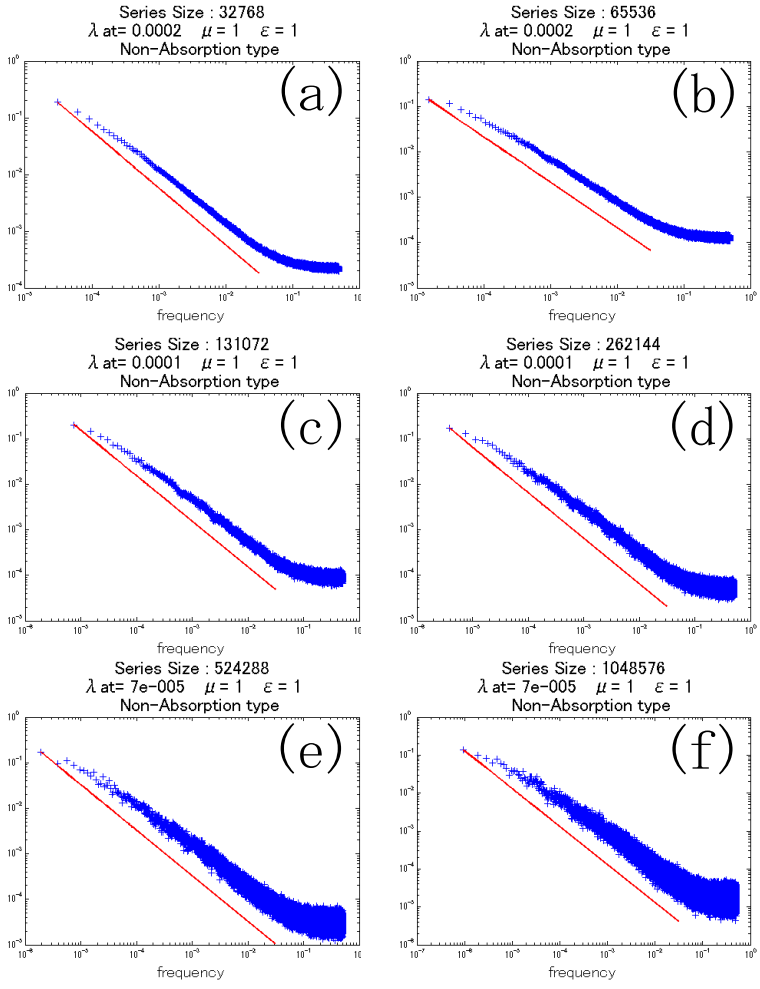

Fig. 14. The PSD of the count series with a non-absorption-type detector for the case of $\mu = 1$ and $\varepsilon = 1$. The particle number limits are 200 in (a) and (b), 400 in (c) and (d), and 700 in (e) and (f), respectively. The series sizes are (a) 32768, (b) 65536, (c) 131072, (d) 262144, (e) 524288 and (f) 1048576, respectively. The straight lines give the f^{-1} behavior.

The above simulations show that, up to the series size of 1048576 or more, the PSD behaves like f^{-1} for about five decades of frequency when $\mu = 1$ and $\varepsilon = 1$, but this behavior is found only for shorter series sizes when either $\mu < 1$ or $\varepsilon < 1$. For longer series, in all cases, the PSD deviates from the f^{-1} behavior and converges to a finite value in a low-frequency range. This deviation is sensitive to decreasing of μ much more than to that of ε. The f^{-1} behavior is found for the series size of 524288 in case of $\varepsilon = 0.5$ and is found for the size of 65538 or more even when $\varepsilon = 0.1$. On the other hand, even in case of $\mu = 0.99$ the PSD deviates from the f^{-1} behavior at the series size of 262144 and, when

$\mu = 0.9$, it deviates at a much more shorter size of 8192. This f^{-1} behavior is gone out rapidly with decreasing μ. These results mean that a time interval between successive particle detections has considerably strong correlation with another time interval for long time when the parameters $\mu = 1$ and $\varepsilon = 1$, and the correlation becomes weaker with decreasing of these parameters, in particular, of the parameter μ.

The detector type has no noticeable influence on the results.

As can be seen in Fig. 1, in case of $\mu = 1$, the existing particle numbers have very strong correlations each other during several hundreds of the mean lifetime of a particle by absorption, and so a time interval between successive particle detections may have also considerable strong correlation with another time interval for long time. When $\mu = 1$ but $\varepsilon < 1$, the correlation between time intervals of successive detections becomes weaker compared with the cases of $\varepsilon = 1$, because the time period between two successive detections is longer for $\varepsilon < 1$ compared to that for $\varepsilon = 1$, which can be seen in Figs. 5 and 6 or Figs. 9 and 10 where the series sizes behaving like f^{-1} are shorter in cases of $\varepsilon < 1$ than in case of $\varepsilon = 1$. When $\mu < 1$, the correlation between the existing particle numbers is strong only for several mean life times which can be seen in Fig. 2, which is the reason why the f^{-1} behavior breaks off at a very short series as shown in Figs. 7, 8, 11 and 12.

When $\varepsilon > 1$ with a non-absorption-type detector, the PDS behavior is similar to the cases of $\varepsilon = 1$ as shown in Fig. 13.

There are at least two limitations on performing the computer simulations. The existing particle number should be avoid to be zero, because no branching will arise from no particle. A very large number of particles takes unreasonably long time to process on a computer, and the number of particles should be set a limit. In the present simulations, the maximum number of particles was set a limit to 1000. The effect of a limitation on the particle number to the PDS was simulated, the results of which is shown in Fig. 15 where the count series were generated under the same conditions of the parameters μ and ε as in Fig. 9 but the particle number limits were set to 200, 400 and 700. As can be seen in Fig.15, the maximum number of particles is so sensitive to the frequency range with the f^{-1} behavior of PDS, where the frequency ranges with the f^{-1} behavior increase steadily with the maximum particle number. This figure shows clearly that the frequency range with the f^{-1} behavior of PDS can be extended more when the simulation is performed for the maximum number of particles larger than 1000. It is not sure that this trend in Fig.15 keeps on and on without limit but, if the maximum number of particles is limited up to 2000, the PDS may behave like f^{-1} for about eight decades of frequency.

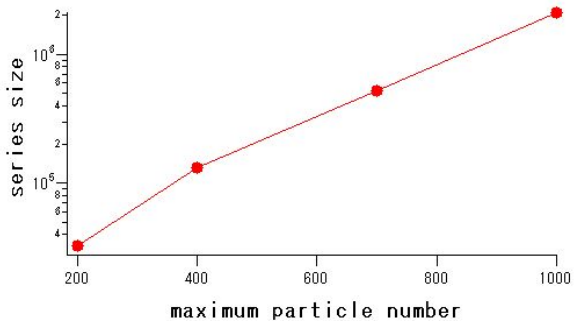

Fig. 15. Relation of the longest series size with the f^{-1} behavior and the maximum number of particles.

In order to see the above expectation, a count series for the maximum number of particle set to 2000 was generated for the case of $\mu = 1$ and $\varepsilon = 1$ with a non-absorption-type detector, the results of which are shown in Fig. 16. It was difficult to generate a fully long series because of a limited computing time, and so the statistical precision of the FFT results in Fig. 16 is insufficient. It can be said still that the PSD behaves like f^{-1} over seven decades of frequency. From the discussions of a limitation of the particle number, the f^{-1} behavior of the PSD over a much more wide frequency range may be expected if a higher-speed computer is used for simulation.

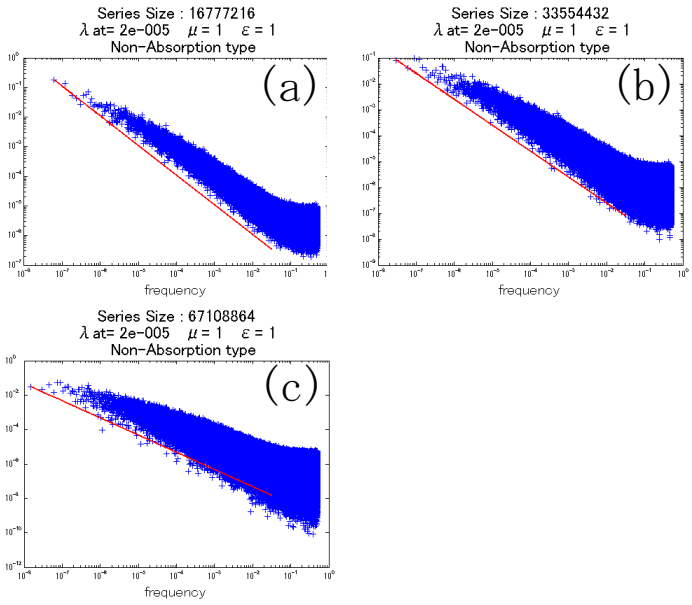

Fig. 16. The PSD of the count series with a non-absorption-type detector for the case of $\mu = 1$ and $\varepsilon = 1$. The maximum number of particles is set to 2000. The series size are (a) 16777216, (b) 33554432 and (c) 67108864. The straight lines give the f^{-1} behavior.

In all of the results of the present simulations, the PDS converges to a finite value in a high-frequency range. The time interval between two successive detections is given digitally in the present work, which may causes interval fluctuation in one time unit, which can be the reason of the behavior of the PDS in a high-frequency range.

5. Conclusion

The branching process model has been applied to discuss a f^{-1} problem, and the f^{-1} behavior of the PDF of a series has been demonstrated in a wide range of frequency, as wide as seven decades of frequency when the absorption rate is equivalent to the branching rate, i.e., μ =1 (critical case). This frequency range may be extended up to eight decades or more by simulating on a higher-speed computer.

References

(1) T. Kobayashi, previous work; $1/f$ *distribution : Branching Process Model (I) ; Formalism,*

(2) T. Kobayashi, *J. Phys. A: Math. Gen.,* **21**, 3723 (1988).

(3) T. Kobayashi, *J. Phys. A:Math. Gen.*, 23, L741 (1990).